Nationaal Lucht- en Ruimtevaartlaboratorium
National Aerospace Laboratory NLR

NLR-TP-2000-228

Turnaround time and accuracy evaluation of viscous flow computations on hybrid grids

J.W. van der Burg, K.M.J. de Cock and S.P. van der Pijl

.

Nationaal Lucht- en Ruimtevaartlaboratorium
National Aerospace Laboratory NLR

NLR-TP-2000-228

Turnaround time and accuracy evaluation of viscous flow computations on hybrid grids

J.W. van der Burg, K.M.J. de Cock and S.P. van der Pijl

.

This investigation has been carried out partly under a contract awarded by the European Commission, contract number BRPR-CT98-4111, and as part of NLR's basic research programme, Workplan Number A.1.B.2.

This report is based on a presentation (to be) held on the European Congress on Computational Methods in Applied Sciences and Engineering ECCOMAS 2000, Barcelona, Spain on 11-14 September 2000.

Division: Fluid Dynamics
Issued: May 2000
Classification of title: unclassified

Abstract

Hybrid grid technology has become an important tool for aerodynamic analysis and design because of the high level of automation. At NLR the FASTFLO CFD system[1] for computing viscous flows around complex aircraft configurations is deployed in aerodynamic project work. Rapid increases in parallel computer architectures, with large aggregate memory capacity and CPU power, allow the application of this CFD technology to even more geometrically complex aircraft configurations. In the paper an overview is presented of the current capabilities of the FASTFLO CFD system among which are three-dimensional hybrid grid generation, viscous flow modelling and grid adaptation. Due to the high level of automation of the CFD system and the focus on geometrically complex aircraft configurations the work on CAD-modelling has increased. Special attention will be devoted towards difficulties encountered in CFD-geometry modelling. To illustrate the capabilities of the FASTFLO CFD system two examples of aircraft configurations are presented.

[1] The FASTFLO CFD system has been developed in the frame of the DLR-NLR co-operation "CFD for Complete Aircraft"and the Brite-Euram fourth framework projects FASTFLO I and II, see references [1-3].

Contents

(20 pages in total)

1 Introduction

Viscous flow calculations for complex aircraft configurations have become feasible due to the application of hybrid grid technology. A short CFD problem turnaround time for complex aircraft configurations has been realised due to introduction of unstructured grid generation techniques which allow a higher level of automation in comparison with the more commonly used, conventional multi-block grid generation techniques.

At the National Aerospace Laboratory NLR the FASTFLO CFD system is available which is based on hybrid grid technology. The FASTFLO CFD system is being exploited in an increasing number of aerodynamic projects. In this paper capabilities of the individual algorithms in the FASTFLO CFD system are addressed and examples of turbulent viscous flow are presented.

2 CFD geometry-modelling

In an aerodynamic project the CAD-geometry of an aircraft configuration is usually received from an aircraft manufacturer. To be able to carry out a CFD analysis for a geometrically complex aircraft configuration it is of importance to analyse and understand the aerodynamic geometry. In the geometry of an aircraft many wanted and unwanted details can be present, such as for instance: finite trailing edges, small holes and gaps, small curves, small surfaces patches, sharp angled surface patches. Before carrying out a CFD analysis these geometrical issues have to be handled.

Based on such a geometric analysis aerodynamically relevant and non-relevant parts of the geometry are identified. It can be decided to locally modify the geometry and to remove unwanted small-scale geometric features. A critical issue that then still remains is the accurate CAD modelling of the geometry. In order to understand this better the concept of CFD-geometry is introduced here.

2.1 From a general CAD geometry to a CFD geometry

The starting point of the FASTFLO CFD system (see figure 1) is a geometry definition which from now on is referred to as the **CFD geometry**. The CFD geometry is defined as the CAD-geometry that consists of a collection of surfaces and trim curves describing all relevant aerodynamic parts and that is topologically and also preferably physically airtight.

Various ‘sending’ CAD systems are used nowadays by aircraft manufactures to define a general CAD/CAM geometry of an aircraft configuration and various ‘receiving’ systems are used to prepare a CFD-geometry. At NLR ICEM CFD and a CAD-interface algorithm are utilised to produce a CFD-geometry. In CAD systems, cloud of points, drawings, or existing geometry definitions can be used to generate, reshape, add, delete, intersect and trim surface patches, such that an airtight CFD geometry results.

A property of the FASTFLO CFD system is that the CFD-geometry should contain information concerning the relation between the curves and surfaces in the geometry often referred to as topological information. In general three methods exist to produce this topological information:

1) By a 'sending' CAD system, for instance by means of a solid model that contains the relevant topology information.
2) Interactively by hand using a CAD system (trimming surfaces).
3) Automatically, by algorithmically adding topology information to the CAD geometry.

For the FASTFLO CFD system a combination of methods 2 and 3 has been pursued. Modern solid modelling CAD systems (currently under development) are able to deliver topological information (and airtight surfaces) and therefore are potentially an interesting alternative (method 1).

Human factors can also play a role in preparing a CFD-geometry. The degree of familiarisation with the geometry requirements of the 'receiving' system (e.g. the CAD system or the CFD system) and the CAD skills of the CAD-specialist are a critical success factor in preparing the CFD geometry. Since a lot of CFD groups do not have these 'in-house' CAD capabilities the process of creating a CFD geometry out of a CAD-geometry is merely an impossible task. Therefore, much emphasis has been placed on the relaxation of the geometry input requirements of the FASTFLO CFD system.

2.2 Geometry exchange leading to geometry change

Care should be taken when exchanging a geometry definition between a 'sending' and ‘receiving' system. Due to geometry exchange the geometry may be modified for several reasons[4].

First, different values in the ‘sending’ and the ‘receiving’ system may have been used for the same point tolerance and for the tolerances in the mathematical representations of curves and surfaces. Tolerances are usually not exchanged in geometry definition files. This problem has particularly a pronounced effect when the geometry consists of geometrical features within the order of the same point tolerance (for instance, a wing trailing edge with finite thickness). The ‘receiving’ system can then interpret these geometric details as non-relevant (within tolerance).

Furthermore, differences can exist in the supported mathematical representations. For instance, the 'sending' system uses NURBS surfaces of a higher order than the maximum order supported by the 'receiving' system. This results in an unwanted change of the CAD-geometry.

Another problem is that a translation by the 'receiving' system of non-supported entities of the 'sending' system, introduces approximation errors or even unstable parameterisations in the translated geometry. The latter can happen for degenerate patches. Due to translation of CAD data round-off errors can be introduced so that geometry does not remain airtight any longer. Geometry curves and/or surfaces can overlap and/or intersect.

These geometric changes have to be recognised and repaired by hand.

2.3 CFD-geometry: possibilities and requirements

The FASTFLO CFD system supports a large range of CFD geometries as input. The CFD geometry can be defined either by the CAD data format IGES 5.1 or by the multi-block based format (structured surface patches).
The CFD geometry is allowed to consist of a large number of curves and surface patches. Typically, in a complex aerodynamic configuration the number of surfaces is in the range of 200-1000. In figures 2 and 3 examples are shown of complex CFD-entities that are triangulated. The number of surfaces for these configurations is 142 and 480 respectively. The colours in these figures signify individual surfaces. The number of curves is approximately in the range of 4-6 times the number of surfaces.

Table 1 IGES 5.1 geometry entities supported by the FASTFLO CFD system

Entity number	IGES 5.1 geometry entity
0	the null entity
102	composite curve
110	a line
112	a spline curve
114	a spline surface
118	a ruled surface
124	the transformation entity
126	a NURBS curve
128	a NURBS surface
142	a curve on a trimmed parametric surface
144	a trimmed parametric surface

Among the geometric options that are supported in the IGES 5.1 CFD geometry are singly and doubly curved NURBS surfaces which can either be trimmed or untrimmed; see Table 1 for a list of supported IGES 5.1 entities.

Especially, the option that allows untrimmed surfaces in a CFD geometry has alleviated the work of the CAD-specialist so that geometrically more complex configurations can be considered in the same time frame. Surfaces in the geometry definition that are intersecting, for instance a wing-body junction or a wing-pylon junction, should be trimmed (IGES 5.1 entity 144).

Small-scale geometric features are allowed in the CFD geometry. Local tolerances have been introduced in the FASTFLO CFD system to support these features. Local tolerances are used to verify distances between points, curves and surfaces. However, geometric features with a scale smaller than the same point tolerance, such as small curves and very small surface patches, should be avoided since these can be interpreted as within tolerance. Therefore it is necessary to decide whether to locally replace these surfaces by larger ones.

As already previously mentioned, the geometry should be topologically and preferably physically airtight. Since, the CFD geometry is approximated by a finite number of curves and surfaces the definition of C^0-continuity is relative: C^0-continuous should be satisfied with respect to a specified small tolerance. The inspection and repair of C^0-continuity can take a few days to complete.

In addition the geometry may consist of a number of unwanted geometric features such as: folded surfaces, gaps and/or holes, single loop curves, surface patches with small angles in the bounding curves, surface patches with highly oscillatory control points (NURBS) and non-relevant geometry inside the aerodynamic geometry. These geometric features have to be removed in order to obtain a suitable CFD-geometry.

2.4 Automatic algorithmic creation of a CFD geometry in IGES 5.1 entities

The CAD interface algorithm in the FASTFLO CFD system checks and verifies the geometric requirements with respect to the CFD geometry defined in the IGES 5.1 format and extracts the geometry topology.

In order to end up with a topological airtight CFD geometry for each pair of neighbouring surfaces an unique curve or chain of curves needs to be detected. For this purpose a trim curve splitting algorithm and an algorithm which verifies the distance between chains of curves is

available. On termination of the algorithm a few curves may still be non-connected (due to a large specified tolerance). An option is offered to connect non-connected curves interactively.

A tight and robust coupling to the IGES 5.1 CAD data format has ensured a large reduction in turnaround time compared to the multi-block approach.

3 Hybrid prismatic-tetrahedral grid generation

In order to be able to compute viscous flows a hybrid grid is generated in the three-dimensional flow domain. On the aerodynamic surfaces as defined by the CFD-geometry a prismatic grid is produced in order to accurately capture the boundary layer. In the remaining part of the flow domain where viscous effects are less dominant a tetrahedral grid is created. The hybrid (prismatic/tetrahedral) grid generation algorithms are suited to handle the following types of aerodynamic configurations: a full model, a half model, a quasi two-dimensional-geometry model, multiple bodies and flat-plate like models. Flow domains representing an internal flow problem can also be handled.

For viscous flow calculations the chosen grid resolution is of major importance. In order to be able to accurately study the aerodynamic features for a specific aircraft configuration the parameters that define the grid should be carefully chosen. This can be a formidable task since a number of grid requirements have to be satisfied.

The first step in the formation of a ‘viscous’ hybrid grid is the surface triangulation of the CFD geometry. The surfaces of the CFD-geometry are approximated by triangles which size is controlled by user-defined sources and/or surface curvature. Important here is that the aerodynamically relevant parts of the CFD-geometry are accurately represented, which implied that firstly the CFD-geometry itself is represented with sufficient accuracy and secondly that sufficient nodes/triangles are used to approximate the aerodynamic effects to be studied.
On parts of the aerodynamic geometry where gradients are large such as on wing leading edges a centrally symmetric surface grid[5] is introduced; Examples of centrally symmetric surface grids can be found in Figures 4 and 8. This option is needed to ensure an accurate viscous flow solution since the discretised gradient and Laplacian operators used in the unstructured flow solver are not invariant for grid-irregularities. The algorithm that produces a centrally symmetric surface grid is based on an advancing line concept. The surface triangles are uniquely orientated such that during prismatic grid generation it is ensured that the prismatic grid advances towards the flow domain.

For reasons of computational efficiency the option exists to reduce the flow domain by specifying a user-defined far field geometry in terms of IGES 5.1 CAD data. This is for instance needed for hypersonic flow problems. The surface triangulation of the far field geometry is then combined automatically with the CFD geometry of the aerodynamic configuration.

To capture the near-wall viscous effects an initial prismatic grid with a uniform height is generated on the aerodynamic surfaces of the aircraft configuration. The uniform height of the prismatic grid D and the height of the first prismatic layer d are calculated from

$$d = 5.893\, y^{+}\, L\, Re^{-0.9}$$
$$D = 0.37\, L\, Re^{-0.2}$$

Here Re is the Reynolds number, L is a geometry scale (such as for instance the chord length) and y^{+} controls the height of the first prismatic layer (usually taken equal to one). The node distribution in the hybrid grid (and thus in the prismatic grid) can be improved later using grid adaptation based on local grid refinement and node movement.
The algorithm to create an initial prismatic grid is based on an advancing layer algorithm that uses an algebraic approach minimising the curvature of the advancing layers. The advancing layer algorithm results in an initial prismatic grid that has a uniform height and that is stretched in wall-normal direction. The prismatic elements are arranged such that the central symmetry property is satisfied[5]. In order to obtain a smooth grid, without inverted elements, the algorithm computes the best marching direction and marching step in each node. In regions of narrow gaps between body components such as a wing and a flap or slat the prismatic grid can be receded automatically in order to avoid grid overlap.
To support accurate viscous flow computations, typically, 30-40 prismatic grid layers are generated. In case more layers are taken a discontinuity in element size between the prismatic grid and the tetrahedral grid occurs. In case fewer layers are specified the wall-normal stretching ratio becomes too large, which leads to a large discretisation error. A difficulty is encountered when the surface grid is clustered. In this case the maximum allowable height of the prismatic grid is reduced.

After prismatic grid generation the non-triangulated planes (symmetry planes and/or far field planes) of the flow domain are triangulated. Starting point for the plane-triangulation algorithm is the specification of boundary planes $x = c_1$, $y = c_2$ and $z = c_3$ and one or multiple surface triangulations describing the aerodynamic configuration and/or the far field geometry. In such a way a full model, a half model, a quasi two-dimensional-geometry model and multiple bodies can be handled in automated manner. As a result of the plane-triangulation algorithm a closed surface triangulation is formed which forms the input for tetrahedral grid generation.

The tetrahedral grid generation algorithm consists of three parts: Generation of an initial tetrahedral grid, automatic node insertion and post-processing. The initial tetrahedral grid that is generated consists of the nodes in the input surface triangulation and some extra nodes needed for boundary recovery. Since the initial tetrahedral grid virtually has no interior grid nodes, the grid consists of a large number of ill-formed tetrahedral elements. Advantage of defining such an initial grid first is that the computing time and memory needed to generate the initial grid is limited and the number of boundary edges and boundary triangles that need to be recovered is also limited.
After the generation of an initial tetrahedral grid, nodes are automatically inserted into the tetrahedral grid based on a user-defined distribution function, which controls the distance between the nodes in the grid. The automatic node insertion algorithm places nodes at the cell centers of tetrahedral elements in the grid until the desired spacing is satisfied. The new nodes are connected to the grid by means of a positive-volume approach that guarantees that the volumes of the elements remain positive. A total memory of approximately 80 words per node is needed for the node insertion algorithm that is the maximum for all grid generation algorithms. In order to ensure a smooth transition of elements between the prismatic grid and the tetrahedral grid extra layers of grid nodes, distributed according to the wall-normal stretching of the prismatic grid, can be inserted into the tetrahedral grid.
Since in the tetrahedral grid sliver elements and non-uniform grid connectivities may be present, the tetrahedral grid should be optimised. The optimisation consists of a redistribution algorithm of the tetrahedral elements, which is derived by minimising a functional[6] and an improvement of the grid connectivity by adopting grid transformations.

Short turnaround times for grid generation are guaranteed due to the incorporation of parallel processing in the grid generation algorithms for shared and distributed memory computers based on the MPI-library. The surface triangulation algorithm based on multi-block format triangulates the surfaces of the CFD-geometry in parallel. A load-balancing algorithm based on surface area size is adopted to decompose the workload. The automatic node insertion algorithm has been made suited for parallel processing as well. The decomposition of an initial grid is accomplished by inserting nodes located on planes of constant x. In between the planes of constant x a tetrahedral subgrid is generated. The final tetrahedral grid is obtained by merging the individual tetrahedral subgrids. As a result the time to generate a tetrahedral grid is significantly reduced.

Finally, by merging the prismatic grid and the tetrahedral grid a hybrid grid is formed. To each surface in the CFD-geometry a boundary identification is associated which will be used to select the boundary condition for this surface.

4 Viscous flow calculation and grid adaption

Three-dimensional steady viscous flow in the FASTFLO CFD system is modelled based on the Reynolds-averaged Navier-Stokes equations. To account for turbulence the one-equation Spallart-Allmaras turbulence model and the two-equation k-omega turbulence model are implemented. Transition from laminar to turbulent flow is enforced by means of boundary conditions.
The flow behaviour near boundaries of the flow domain is modelled by means of boundary conditions such as: solid walls on which a laminar or a turbulent boundary layer develops, symmetry plane(s) which reduce the size of the computational domain, far field boundaries and engine inflow and outflow boundaries. An option is also to model inviscid flow with Euler equations and the appropriate wall boundary conditions.

Since viscous flow computations on hybrid (prismatic/tetrahedral) grids for complex aircraft configurations are expensive in terms of computing time a supercomputer is needed to compute the steady viscous flow solution. At NLR the viscous flow computations are carried out on the NEC SX-5/8B supercomputer. This vector-computer possesses eight vector processors and has a shared main memory of 64 Gbyte. The peak speed is 8 Gflops per processor. Due to the edge-based data-structure adopted in the flow solver a good vector and parallel performance is realised on the NEC SX-5/8B.

In the viscous flow solver a steady viscous flow solution is computed by adopting an explicit Runga-Kutta time stepping method. Convergence acceleration is achieved due to application of local time stepping, explicit residual averaging and multigrid based on an agglomeration algorithm. For the spatial discretisation of the convective terms in the Reynolds-averaged Navier-Stokes equations a central or an upwind scheme can be utilised. The convection terms of the k-omega turbulence model can be discretised with first-order or second-order accuracy.

The aerodynamic problem is specified in terms of the onflow conditions (angle of attack, side slip angle), the physical flow model (inviscid or viscous laminar or turbulent flow), the turbulence model, the boundary conditions (engine inlet and outlet conditions), the total extent of the flow domain and a number of transition lines. The precise specification and verification of these items takes at most one day for complex aircraft configurations.
In order to increase the grid resolution of the hybrid grid in regions of the flow domain where gradients are large a grid adaptation algorithm is employed. The grid adaptation algorithm is based on local grid refinement and node movement and utilises an equi-distribution grid adaptation algorithm that ensures that desirable flow features are not overlooked. In order to accurately represent the CFD-geometry after grid adaptation new boundary nodes are projected onto the underlying IGES 5.1 surface of the CFD-geometry. Difficulty here is that due to the projection of a new node badly shaped elements may be formed which are difficult to remove.

As a remedy a linear interpolation of the surface grid is made which locally changes the aerodynamic geometry.

5 POST-PROCESSING and visualisation

For the analysis of a viscous flow solution a post-processing algorithm for large-scale data is available. The post-processing algorithm allows an efficient computation of aerodynamic quantities and coefficients for the aerodynamic configuration under consideration. An advantage here is that the post-processing algorithm is installed on the NEC SX5/8B super computer ensuring short computation times.

Coefficients for lift, side force, pitching moment, yawing moment and rolling moment for the entire aircraft or parts of it can be computed in different coordinate systems: aircraft, stability, wind or a user defined coordinate system.
The post-processing algorithm provides an interface to visualisation software such as TecPlot and EnSight. The distribution of aerodynamic quantities such as for instance the Mach-number, velocity components, pressure coefficient, skin friction and y^+ can be analysed on user-defined sections of the geometry, on pre-specified surface parts of the geometry or in the interior of the flow domain (on slice planes).
Furthermore, the post-processing algorithm provides the possibility to compute local aerodynamic coefficients on sections of an aerodynamic part of the CFD-geometry.

6 Applications

For two aircraft configurations the capabilities of the FASTFLO CFD system are illustrated. For an ONERA M6 wing and an AS28G wing-body configuration a fully turbulent viscous flow calculation is performed with the one-equation Spallart-Allmaras turbulence model. The grid dimensions for each configuration are listed in Table 2. In the viscous flow computations a convergence of three-orders of magnitude in the residual has been realised.

Table 2 Grid dimensions of the hybrid grids

Configuration	Surface Nodes	prismatic layers	nodes
ONERA M6 wing	34899	40	1.7 M
AS28G-wb	52329	40	3.0 M

For the ONERA M6 configuration a centrally symmetric surface grid at the leading edge of the wing is introduced (see Figure 4). The computed surface pressure and skin friction distribution are shown in Figures 5 and 6. The prismatic grid is specified such that the first layer corresponds to approximately $y^+ = 1$ (see Figure 4 and 7) and the height of the last prismatic layer matches the tetrahedral grid. From Figure 7 it can be observed that the computed viscous flow solution is in close agreement with a structured grid viscous flow solution.

For the AS28G wing-body configuration a centrally symmetric surface grid has been introduced at the leading edge of the wing (see Figure 8). The computed surface pressure and skin friction distribution are shown in Figure 9 and 10. The y^+-value for the first layer of the prismatic grid is taken as 2. In Figure 11 it can be seen that agreement with experimental values is obtained (for sections $\eta = 0.229$ and $\eta = 0.477$). At the wing-body junction somewhat higher values for the skin friction are found due the structure of the prismatic grid, viz. an increased height of the prismatic cells. Optionally, transition from laminar flow to turbulent flow is handled by defining a laminar flow region on the leading edge of the wing as shown in Figure 8 (not used in the computation).

7 Conclusions

Due to the introduction of highly automated grid generation algorithms and viscous flow solver algorithms the major workload for carrying out a viscous flow calculation has been shifted towards CFD geometry modelling and aerodynamic post-processing, visualisation. Since the focus for applying hybrid grid technology will be directed to geometrically very complex aircraft configurations the calendar time consumed to prepare a CFD geometry will increase. Therefore the need for improved CAD-capabilities increases.

The viscous flow capabilities of the FASTFLO CFD system have been demonstrated for two aircraft configurations. The CFD-problem turnaround time is in the order of 1-3 days. At NLR the experience is that for geometrically even more complex aircraft configurations the CFD problem turnaround time remains within the order of one week.

Concerning the accuracy of the FASTFLO CFD system it has been demonstrated that the CFD system produces viscous flow solutions which agree well with computational (multi-block structured) and experimental results.

Viscous flow computations for complex aircraft configurations require careful planning. First of all before carrying out the viscous flow computations the CFD specialist should be aware of the

geometric features and fidelity of the geometry definition. Since more complex geometries are handled this step becomes increasingly important. Furthermore, the parameters controlling the hybrid grid generation and the viscous flow solution should be carefully chosen in order to compute an accurate viscous flow solution.

Finally, an interesting and challenging CFD technology has become available which allows the development of future new technologies such as for instance time-accurate viscous flow calculations and fluid-structure coupling systems.

8 References

[1] Burg, J.W. van der; Oskam, B.; Gerhold, T.; Galle, M.; Berglind, T.; Arlinger, B.; Kretzschmar, G.; Haase, W.; FASTFLO Contract No. BRPR-CT96-0184, *Annex 1 Project programme*, NLR CR 96275 L, February, 1996.

[2] Burg, J.W. van der; Oskam, B.; *FASTFLO-Automatic CFD system for the three-dimensional flow simulations, in: Nouvelle Revue Aeronatique, No. 2*, Elsevier, April, 1998.

[3] Burg, J.W. van der; Oskam, B.; Gerhold, T.; Galle, M.; Berglind, T.; Arlinger, B.; Kretzschmar, G.; Haase, W.; Wesseling, P.; *FASTFLO II Project Programme*, NLR TR 98052 L, January, 1998.

[4] Wulf, A., Steberl, R., Akdag, V; "*Efficient integration of CFD into product design", presented at the Industrial Computational Fluid Dynamics conference, VKI, May 1999*.

[5] Burg, J.W. van der, Maseland, J.E.J.; Oskam, B.; *Development of a fully automated CFD system for three-dimensional flow simulations based on hybrid prismatic-tetrahedral grids, in Proceedings of the 5th Int. Conf. on Num. Grid Gen. in CFD and related fields*, Starkville, Mississippi, April, 1996.

[6] Burg, J.W. van der, "*Tetrahedral grid optimisation", in proceedings of the 7th International Conference on Grid Generation in Computational Field Simulation*, Whistler, British Columbia, Canada, September, 2000.

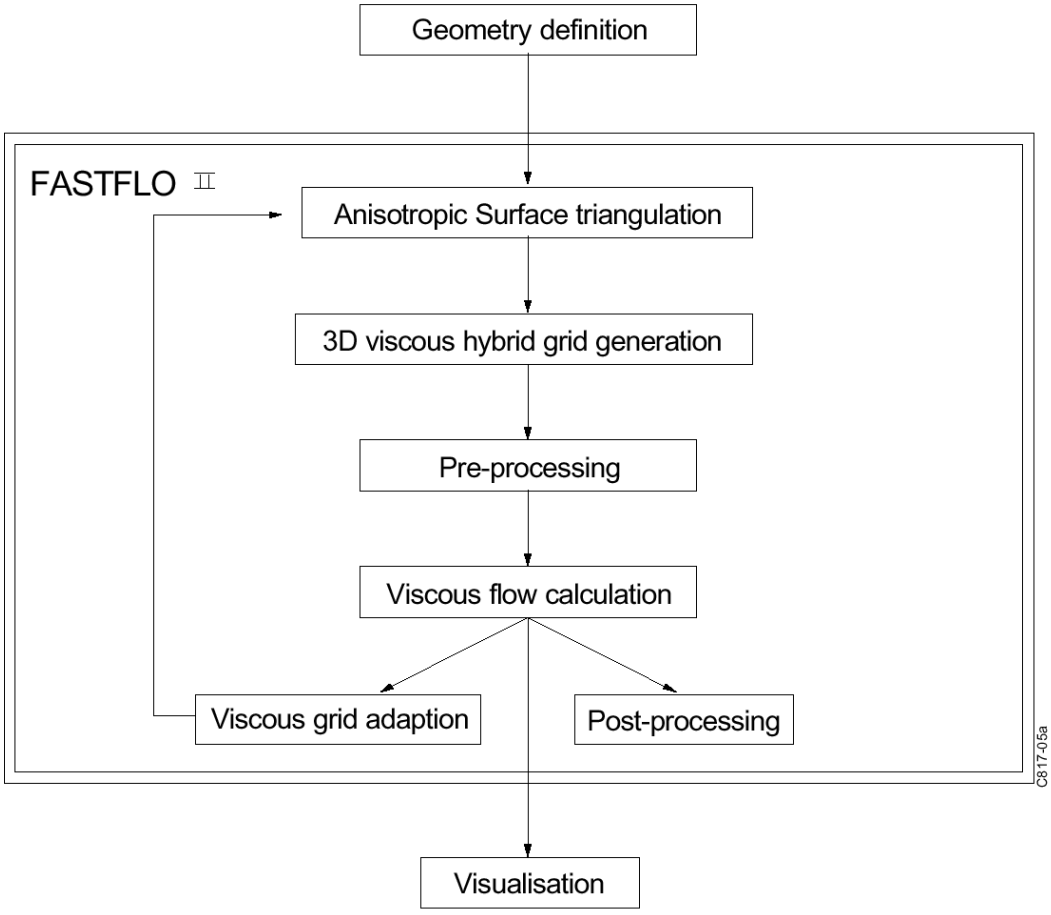

Fig. 1 Overview of the algorithmic components in the FASTFLO CFD system

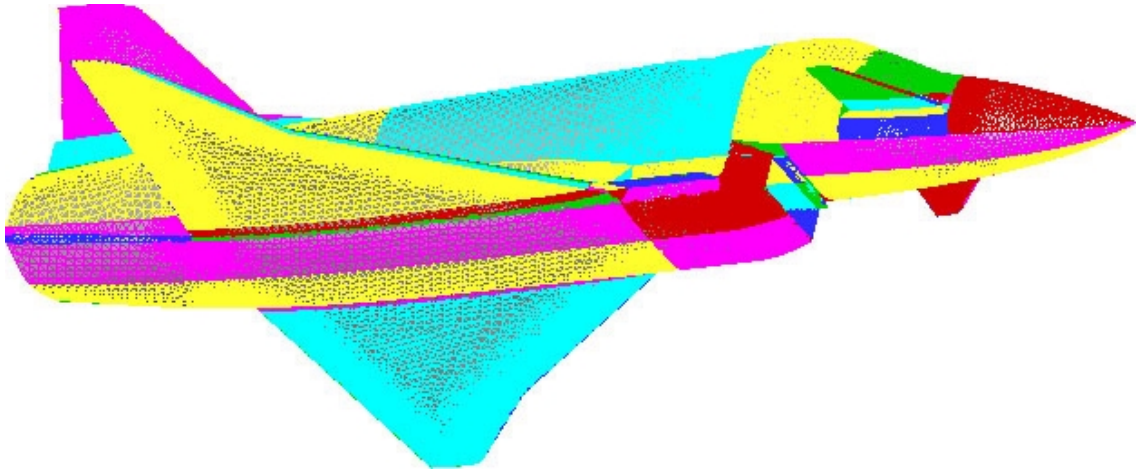

Fig. 2 Surface triangulation of the CFD-geometry for the X31 experimental aircraft

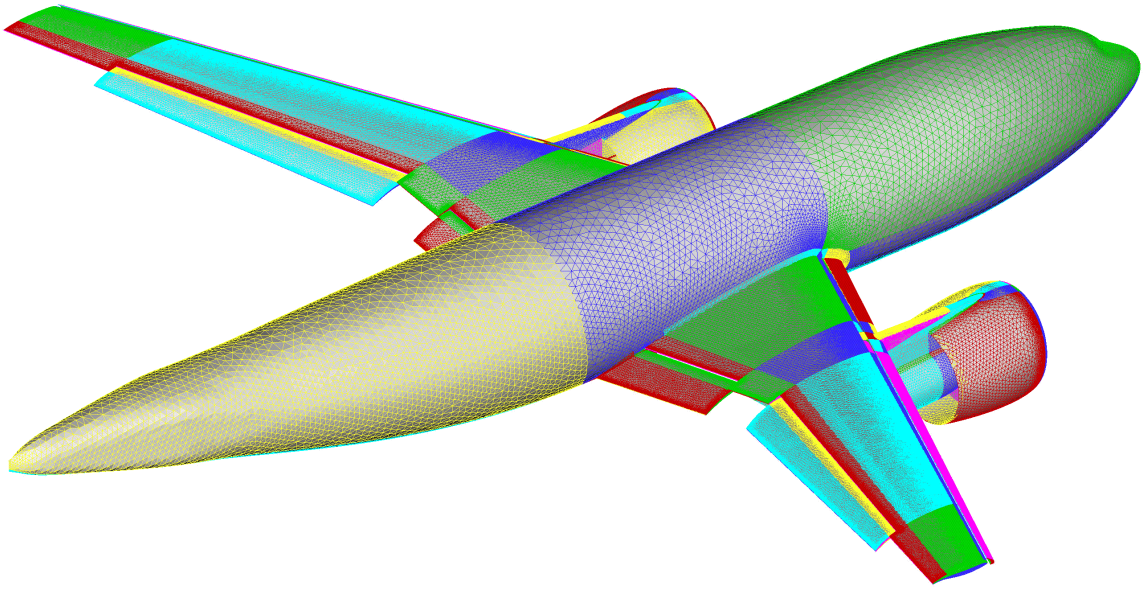

Fig. 3 Surface triangulation of the CFD geometry for the ALVAST high-lift configuration

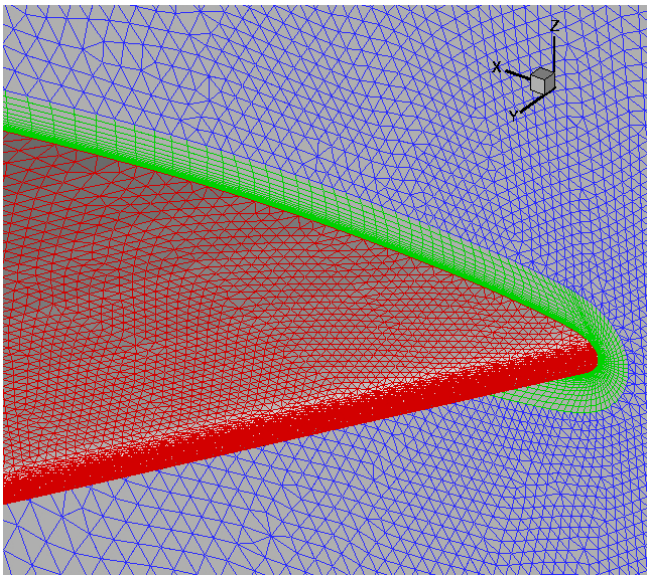

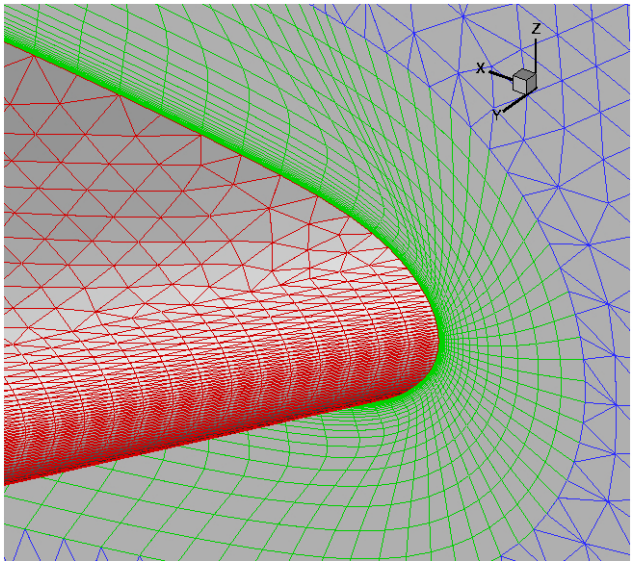

Fig. 4 Surface triangulation of the ONERA M6 wing; close-up of the wing leading edge

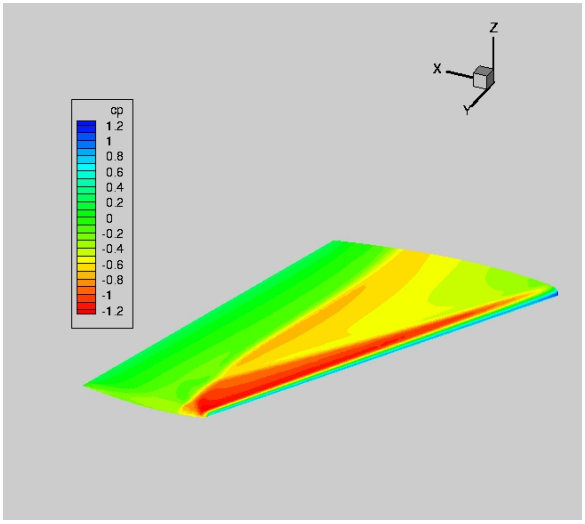

Fig. 5 Pressure coefficient distribution for the ONERA M6 wing

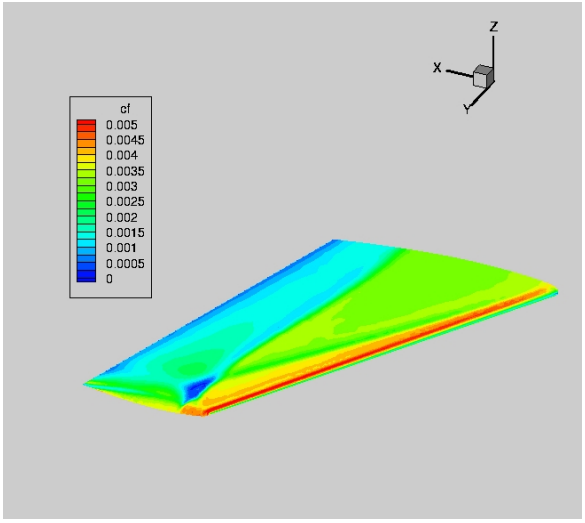

Fig. 6 Skin friction distribution for the ONERA M6 wing

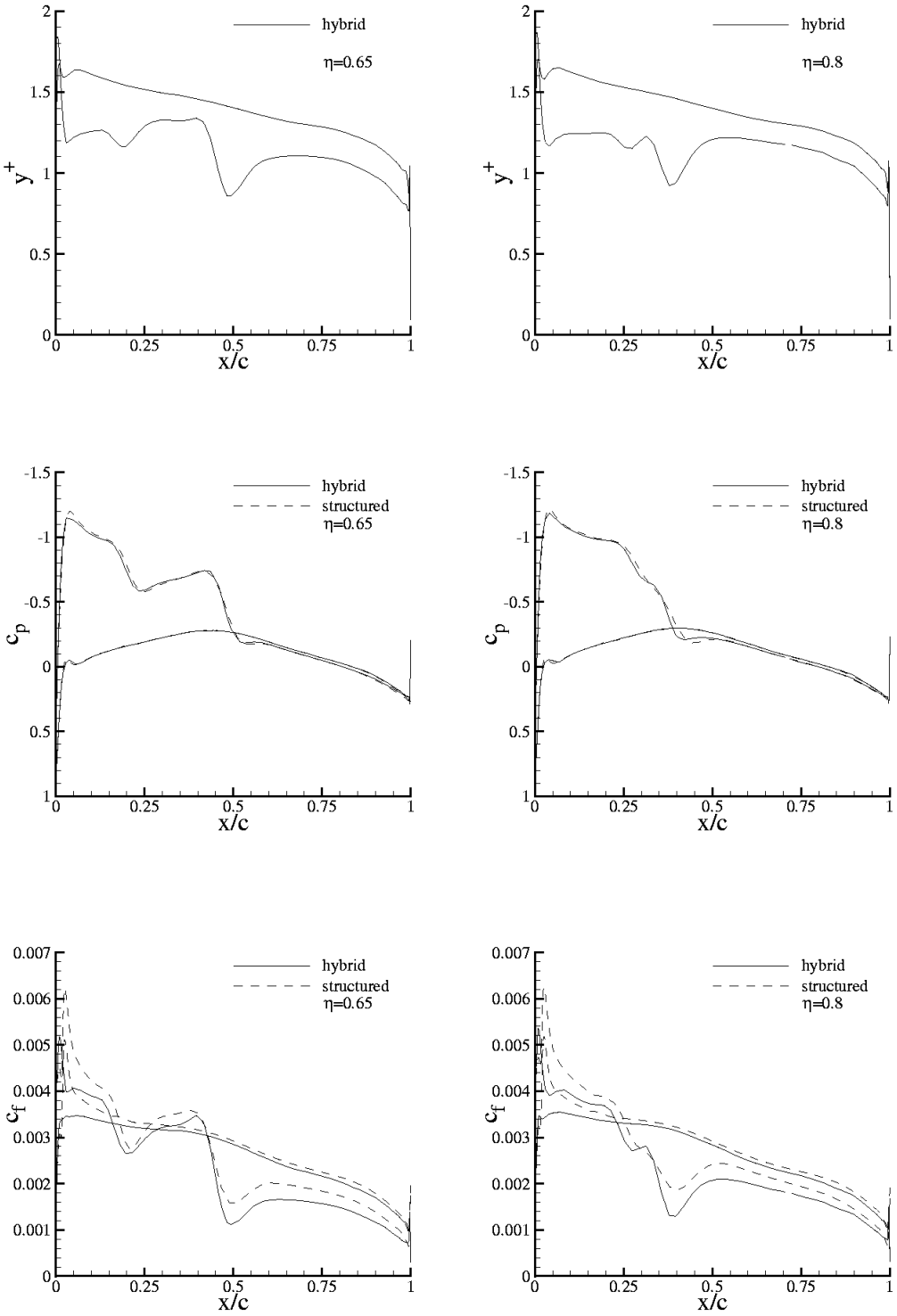

Fig. 7 Comparison of hybrid and structured grid viscous flow solutions for the ONERA M6 wing; Distribution of y^+, pressure and skin friction coefficient for the sections 0.65 and 0.8.

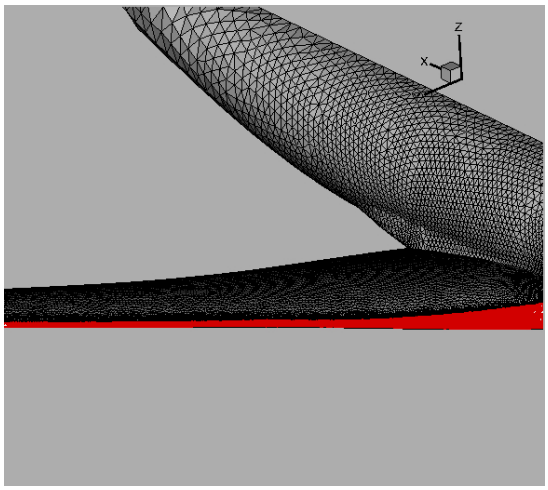

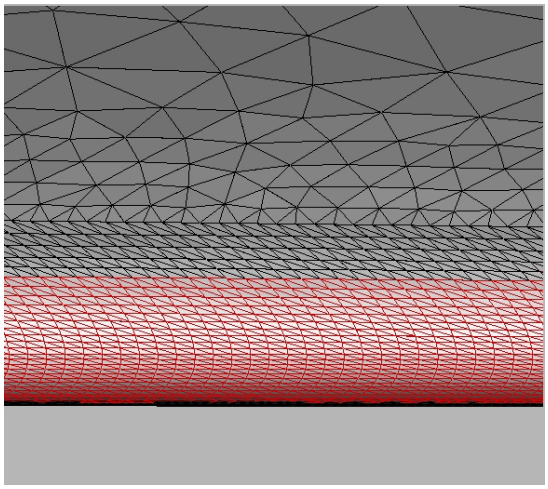

Fig. 8 Specification of the laminar flow region on leading edge of the wing; AS28G wing-body

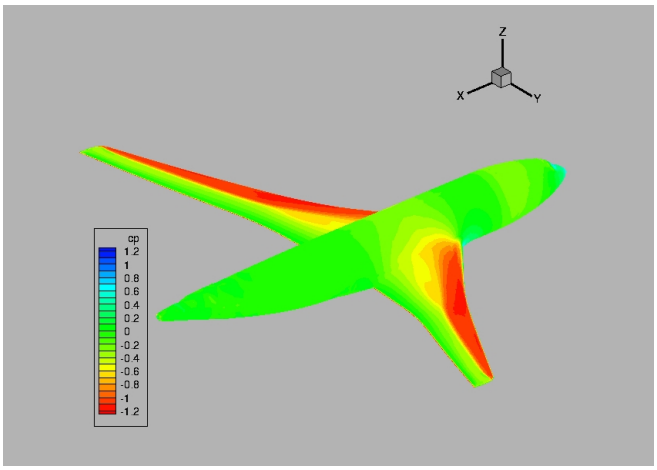

Fig. 9 Pressure distribution for the AS28G wing-body

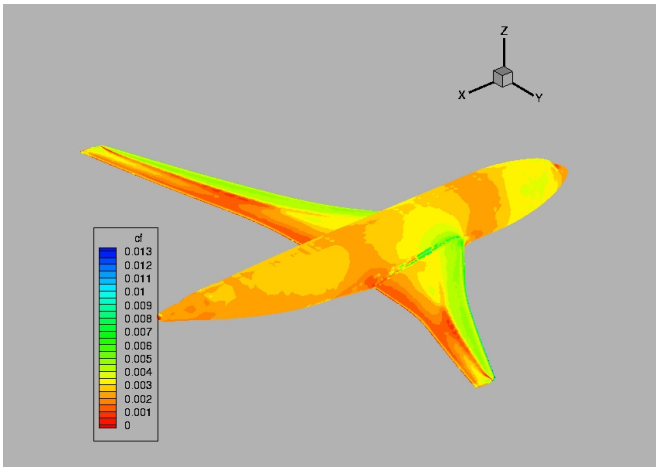

Fig. 10 Skin friction distribution for the AS28G wing body

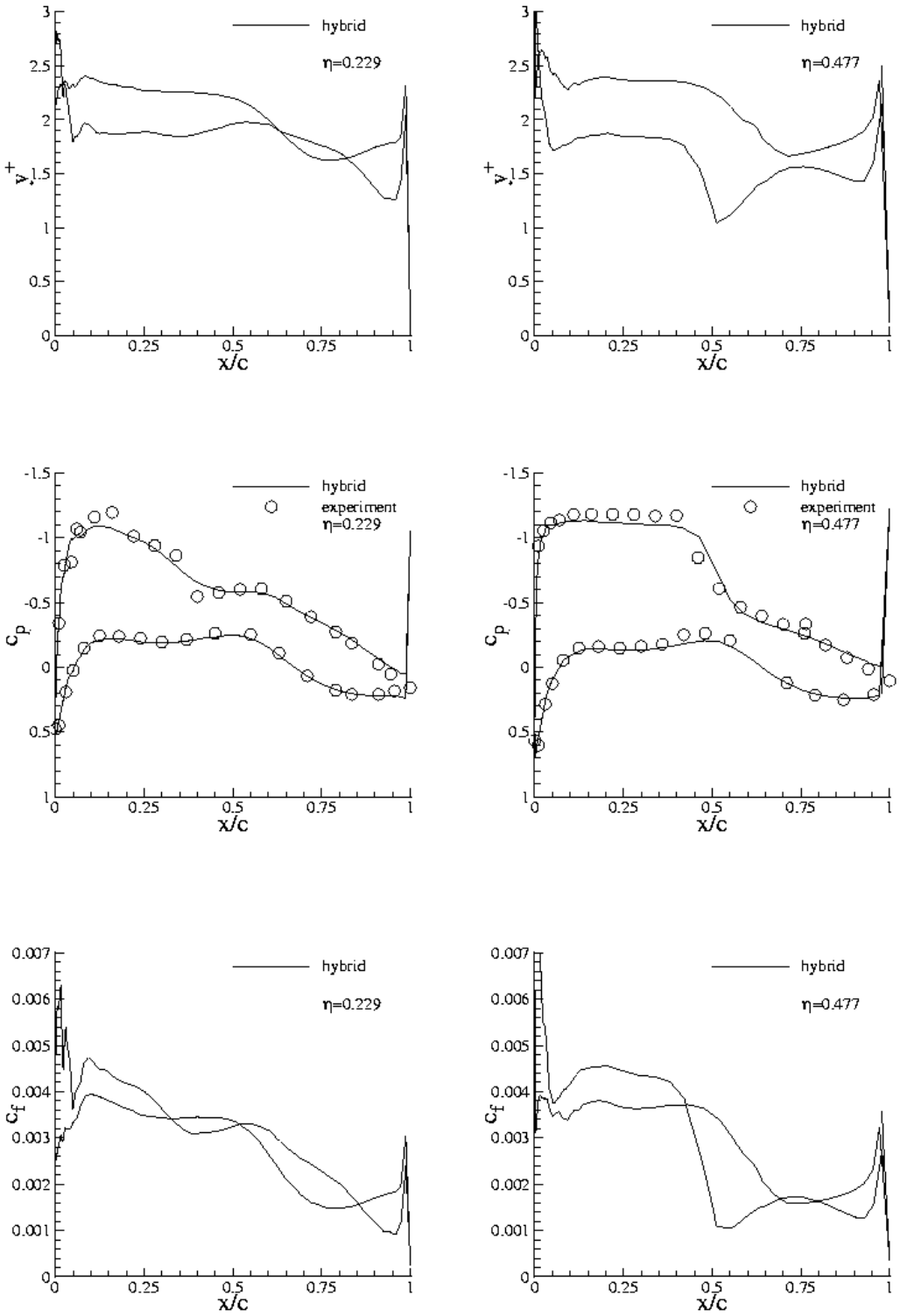

Fig. 11 Comparison of the viscous flow solution and the experiment for the AS28G wing-body; Distribution of y^+, pressure and skin friction coefficient for the sections 0.229 and 0.477.